Ice core records as sea ice proxies: an evaluation from the Weddell Sea region of Antarctica

Nerilie. J. Abram[1], Robert Mulvaney[1], Eric W. Wolff[1], and Manfred Mudelsee[2,3]

1. British Antarctic Survey, High Cross, Cambridge CB3 0ET, United Kingdom.
2. Climate Risk Analysis, Wasserweg 2, 06114 Halle, Germany.
3. Institute of Meteorology, University of Leipzig, Stephanstrasse 3, 04103 Leipzig, Germany.

[1] **Ice core records of methanesulphonic acid (MSA) from three sites around the Weddell Sea are investigated for their potential as sea ice proxies. It is found that the amount of MSA reaching the ice core sites decreases following years of increased winter sea ice in the Weddell Sea, opposite to the expected relationship if MSA is to be used as a sea ice proxy. It is also shown that this negative MSA-sea ice relationship cannot be explained by the influence that the extensive summer ice pack in the Weddell Sea has on MSA production area and transport distance. A historical record of sea ice from the northern Weddell Sea shows that the negative relationship between MSA and winter sea ice exists over interannual (~7 year period), and multi-decadal (~20 year period) time scales. NCEP/NCAR reanalysis data suggest that this negative relationship is most likely due to variations in the strength of cold offshore wind anomalies travelling across the Weddell Sea, which act to synergistically increase sea ice extent while decreasing MSA delivery to the ice core sites. Hence, our findings show that in some locations atmospheric transport strength, rather than sea ice conditions, is the dominant factor that determines the MSA signal preserved in near-coastal ice cores. A cautious approach is thus required in using ice core MSA for reconstructing past sea ice conditions, including the need for networks of ice core records and multi-proxy studies to assess the significance of past MSA changes at different locations around Antarctica.**

INDEX TERMS: 0750 Cryosphere: sea ice (4540); 0724 Cryosphere: ice cores (4932); 9310 Antarctica (4207); 1616 Climate variability (1635, 3305, 3309, 4215, 4513)

KEYWORDS: sea ice, ice core, MSA, Antarctica, Weddell Sea.

1. Introduction

[2] Sea ice is believed to be a vital component in the regional climate and circulation systems of Antarctica [*Cavalieri et al.*, 1997; *Parkinson*, 2004], and also influences ecosystem productivity around the continent [*Atkinson et al.*, 2004]. Systematic satellite measurements of Antarctic sea ice first began in 1973, however the detection of any long-term changes in these sea ice records is hindered by their relatively short time span and the strong interannual to decadal variability of Antarctic sea ice [*Cavalieri et al.*, 1997; *Curran et al.*, 2003; *Parkinson*, 2004]. Longer, but regionally sparse, historical records do provide some evidence for a long-term decline in Antarctic sea ice during the 20th century [*de la Mare*, 1997; *Murphy et al.*, 1995; *Rayner et al.*, 2003]. However, it remains unclear how these changes may have been linked to observational records of 20th century climate change in Antarctica [*Cook et al.*, 2005; *Vaughan et al.*, 2003]. In turn, it is still not clear to what extent Antarctic sea ice may play a role in future changes in climate, both in Antarctica and globally. To address these issues a proxy for reconstructing past sea ice conditions is needed.

[3] Antarctic ice cores are valuable archives of palaeoenvironmental conditions, and ice core records of both sea salt and methanesulphonic acid (MSA; CH_3SO_3H) have been proposed as potential proxies for sea ice [*Welch et al.*, 1993; *Wolff et al.*, 2003]. Sea salt in ice cores has traditionally been viewed as a proxy for transport strength and storminess. However, the observation of increased sea salt in Antarctic ice cores during winter, and during glacial periods, has recently led to suggestions that sea salt may instead reflect the formation of brine and frost flowers on top of new sea ice [*Wolff et al.*, 2003]. Whilst ice core records of sea salt appear to respond to sea ice changes over long time scales (e.g. glacial-interglacial; [*Wolff et al.*, 2006]), this proxy has not yet been shown to be sensitive to sea ice production over interannual to century time scales. The other potential sea ice proxy, MSA, is derived ultimately from marine phytoplankton productivity at the sea ice margin [*Kawaguchi et al.*, 2005]. During spring and summer, the decay

of sea ice enhances the activity of these phytoplankton that produce dimethylsulphide (DMS; $(CH_3)_2S$) [*Curran and Jones*, 2000]. DMS is released to the atmosphere where it is rapidly oxidised to form MSA [*Ravishankara et al.*, 1997]. This is the only known source of MSA in Antarctic ice cores, leading to theories that MSA records from near-coastal ice cores could provide reconstructions of past biological activity and sea ice conditions [*Curran et al.*, 2003; *Saigne and Legrand*, 1987].

[4] Comparisons of Antarctic ice core MSA records with instrumental records of sea ice have produced varying results. For example, an MSA record from Dolleman Island on the eastern Antarctic Peninsula was found to have a negative correlation with a historic record of winter sea ice duration at the South Orkney Islands [*Pasteur et al.*, 1995]. A negative correlation was also found between an MSA record from Lambert Glacier [*Sun et al.*, 2002] and more recent satellite records of winter sea ice area in the Indian Ocean sector. In contrast, positive correlations have been identified between regional satellite records of annual sea ice area and ice core MSA from Newell Glacier [*Welch et al.*, 1993] and, more recently, between winter sea ice extent and MSA at Law Dome [*Curran et al.*, 2003]. The Law Dome study found that strong decadal cycles in sea ice extent had masked long-term changes in the relatively short satellite records, and the ice core MSA results were used to infer that winter sea ice extent in the Law Dome region had decreased by around 20% since the 1950s [*Curran et al.*, 2003].

[5] The potential for sea ice reconstructions that was demonstrated by the Law Dome MSA record now needs to be tested at other locations. The varying results of earlier studies suggest that the link between ice core MSA records and sea ice is not the same at all sites around Antarctica, and accordingly not all ice core MSA records may be suitable as sea ice proxies. In this study we use the MSA records of three near-coastal ice cores from sites around the Weddell Sea to examine MSA-sea ice relationships in a region with a distinctly different sea ice regime to the Law Dome

site (Fig. 1). The sea ice-MSA relationship in the Weddell Sea region is first examined using a range of sea ice parameters from post-1973 satellite records of sea ice. The natural variability of MSA and sea ice in this region are then further assessed using a historical record of sea ice duration from the northern Weddell Sea that begins in 1903. This study thus allows for a detailed evaluation of the nature and drivers of MSA variability in the Weddell Sea region and, in turn, the factors that need to be considered in assessing the suitability of Antarctic ice core MSA records as sea ice proxies.

2. Ice core sites and analysis

[6] The ice cores used in this study were collected by the British Antarctic Survey from three sites around the margin of the Weddell Sea (Table 1; Fig.1); Dolleman Island [*Pasteur et al.*, 1995], Berkner Island [*Mulvaney et al.*, 2002] and Dronning Maud Land (DML). Snow accumulation at these sites is generally associated with low pressure systems that have either tracked across the Weddell Sea from the southern Atlantic Ocean, or that have developed over the Weddell Sea due to blocking by the Antarctic Peninsula [*Noone et al.*, 1999; *Reijmer et al.*, 1999; *Reijmer and van den Broeke*, 2000; *Russell et al.*, 2004]. Backwards trajectory analysis shows that the Dolleman Island site, on the western margin of the Weddell Sea, is also influenced by air masses that have travelled over the Antarctic Peninsula from the Amundsen-Bellingshausen Seas and the southern Pacific Ocean [*Russell et al.*, 2004].

[7] The ice cores were shipped frozen to the United Kingdom where they were subsampled using a bandsaw that had been cleaned with frozen ultra-pure water. The Dolleman Island core was subsampled at a resolution of approximately 12 samples per year. Following high-resolution analysis of major ions, aliquots of the Dolleman Island subsamples were combined to produce annual samples for MSA analysis [*Mulvaney and Peel*, 1988; *Pasteur et al.*, 1995]. Subsampling

of the Berkner Island core was carried out at annual resolution, as defined by electrical conductivity measurements (ECM). The DML core was subsampled at psuedo-annual resolution based on modern day snow accumulation rates and ice densification modelling. The chronologies of each of the cores were further constrained using volcanic stratigraphic markers recorded in non-sea salt SO_4^{2-} and electrical profiles, and β-radioactivity peaks caused by nuclear weapons testing [*Hofstede et al.*, 2004; *Mulvaney et al.*, 2002]. In the case of the DML core these fixed stratigraphic markers were used to refine the ice densification model for this site and provide more reliable age estimates for the pseudo-annual samples. For the purposes of this study, the DML data was then linearly interpolated to provide an annually averaged timeseries. It is estimated that the annual dating of the ice cores is accurate to ± 1 year during the satellite era (post 1973), and accurate to within ± 2 years back to the start of the 20th century.

[8] In the Berkner Island and Dolleman Island cores the annual samples defined by ECM and major ion analyses run from winter to winter, and are thus centred around the austral summer peak of MSA [*Minikin et al.*, 1998]. The interpolated annual averages of the DML data are also centred on the austral summer, and any signal smoothing caused by the original pseudo-annual sampling method should not significantly affect the interannual variability examined in this study. MSA has been shown to experience post-depositional loss in snow, and further diffusional movement in ice [*Mulvaney et al.*, 1992]. Interpreting interannual variations in MSA as an environmental signal uses the assumption that post-depositional MSA loss in the snow pack remains approximately constant over time, and so does not disturb the ice core MSA anomaly related to environmental processes [*Fundel et al.*, 2006]. Later disturbance of the environmental MSA signal due to migration in ice appears to be restricted to sub-annual scales in late Holocene ice cores [*Curran et al.*, 2002; *Pasteur and Mulvaney*, 2000], and thus MSA migration should not be a significant source of error for the annual MSA samples used in this study. MSA was measured for the Weddell region ice core

samples by ion-chromotography, using Dionex instruments and columns. Typical precision of the MSA measurements using this system is ±5%.

3. The satellite era (post-1973)

3.1 Satellite sea ice datasets

[9] The first sea ice dataset used to examine MSA-sea ice relationships in the Weddell region ice cores was derived from Joint Ice Centre (JIC) maps. These maps show the latitude of the sea ice edge (defined as 15% sea ice cover) for 10 degree sectors of longitude around Antarctica. The JIC maps record weekly sea ice extents (SIE) from 1973 to 1996, and have been compiled into monthly SIE summaries [*Jacka*, 1990].

[10] The other satellite sea ice dataset used in this study is derived from NASA scanning multichannel microwave radiometer (SMMR; 1978 – 1987) and special sensor microwave/imager (SSM/I; 1987 – 1998) instruments [*Comiso*, 1999; *Zwally et al.*, 2002]. The NASA sea ice data begin almost six years after the JIC records, and thus the period for calibrating with the ice core MSA records is shorter. The NASA dataset used here also does not have the same longitudinal resolution as the JIC data, instead being compiled into 5 broad regional areas around Antarctica [*Zwally et al.*, 2002]. However, the NASA data are based upon cumulative sea ice conditions throughout the sea ice pack and, unlike the Jacka/JIC data, are able to incorporate features such as open water areas within the ice pack and latitudinally-oblique ice edge geometry that exist in the Antarctic Peninsula and Weddell Sea regions. In the NASA dataset, SIE is defined as the cumulative area of all grid cells having at least 15% sea ice concentration, while ice covered area (ICA) is the sum of area multiplied by sea ice concentration for each grid cell [*Zwally et al.*, 2002]. In this study we use the bootstrap algorithm version of the NASA sea ice data as this has been

shown to produce the best fit between satellite and sonar sea ice data for the Weddell Sea [*Connolley*, 2005].

[11] Theories of the MSA-sea ice relationship involve phytoplankton blooms that occur during the break-up of winter sea ice. Following the method of Curran *et al.* [2003], August-October averages of the satellite sea ice data were used to define the winter maxima in sea ice conditions (SIE_{max} and ICA_{max}). These winter sea ice conditions were then compared with annual averages of ice core MSA centred on the following austral summer. However, the persistence of sea ice throughout summer in the Weddell Sea means that the winter maximum in sea ice may not be best measure for examining MSA-sea ice relationships in this region. Because of this we also compared our ice core MSA records to time series of the January-March minimum in sea ice conditions (SIE_{min} and ICA_{min}), and to the amount of sea ice decay each year (decay = max – min).

3.2 Features of the post-1973 ice core MSA records

[12] The three ice core records from the Weddell Sea region exhibit a large range in mean MSA concentrations (Table 1). In the post-1973 period (satellite era) the DML core has a mean concentration of 4.9 μg/kg (ppb), which is similar to that of the Law Dome ice core record (6.5 ppb; [*Curran et al.*, 2003]). Mean MSA concentrations rise to 16.6 ppb for the Berkner Island core and to 55.4 ppb for the Dolleman Island core. It has previously been suggested that the exceptionally high MSA concentrations in Dolleman Island ice reflect a large local source of MSA to this site [*Mulvaney et al.*, 1992; *Pasteur et al.*, 1995]. The decrease in MSA concentration with increasing altitude and distance from the coast that is observed in these three ice cores (Table 1) is not an unexpected result, as atmospheric concentrations of MSA can decrease by a factor of two over transport distances of a few hundred kilometres [*Minikin et al.*, 1998; *Minikin et al.*, 1994].

[13] Despite differences in mean MSA concentrations, the three ice core MSA records show similar patterns of interannual variability during the satellite era (Fig. 2a). In order to reduce the effects of noise in the individual ice core records and better isolate the common regional MSA signal, the three ice core MSA records were normalised and then averaged to produce a single post-1973 stacked MSA record for the Weddell Sea region (Fig. 2b). Interannual variability in the MSA records was compared with the satellite records of sea ice using linear correlation analysis. Significance levels for the correlations were estimated using a 2-tailed t-test, with an AR(1) persistence correction for effective sample size [*von Storch and Zwiers*, 1999].

3.3 Correlation of ice core MSA with satellite sea ice records

[14] The three individual ice core MSA records all show negative correlations with the winter maximum in sea ice conditions in the Weddell Sea (i.e. increased MSA corresponds to reduced winter sea ice; Fig. 3b; Table 2). This negative correlation is strongest for the Berkner Island and DML cores, where negative correlation values persist across the entire Weddell Sea sector. For the Dolleman Island MSA record, the negative correlation is observed only at the western margin of the Weddell Sea (Fig. 3b). The common negative relationship between ice core MSA and winter sea ice becomes clearer using the stacked MSA record. Using the JIC data (Fig. 3a) negative correlations are observed with winter sea ice extents throughout the Weddell Sea, with the correlation peaking between 0-10ºW (r = -0.50). This finding is confirmed using the NASA sea ice dataset for the Weddell Sea sector, where significant negative correlations are observed for winter sea ice extent and area (Table 2; r_{SIE} = -0.76, r_{ICA} = -0.78). It is important to note that this negative relationship between ice core MSA and winter sea ice in the Weddell Sea region is opposite to the positive regional correlations produced by this method for the Law Dome/western Pacific sector of Antarctica [*Curran et al.*, 2003].

[15] The Weddell region MSA records do, however, show significant positive correlations with winter sea ice in the more distant Amundsen-Bellingshausen Seas. Using the JIC winter sea ice extent data this positive correlation is found to peak at 90-100ºW (Fig. 3a; r = +0.62). Similar results are again produced using the NASA winter sea ice data for the Amundsen-Bellingshausen Sea sector (Table 2; r_{SIE} = 0.62, r_{ICA} = 0.62).

[16] Comparison of the ice core MSA records with the summer sea ice minimum and with sea ice decay do not produce strong, regional correlation patterns like those observed with the winter sea ice maximum. Summer sea ice in both the Weddell Sea and Amundsen-Bellingshausen Seas has generally positive correlations with our ice core MSA records, however these correlations are not statistically significant (Fig. 3c). Sea ice decay produces the same correlation pattern as observed using the winter sea ice maximum (i.e. negative correlations in the Weddell Sea, positive correlations in the Amundsen-Bellingshausen Seas; Fig 3d), however the overall correlations are not as strong or regionally extensive as observed for winter sea ice. The negative correlations between the NASA record of sea ice decay in the Weddell Sea and the stacked MSA record are statistically significant (r_{SIE} = -0.67, r_{ICA} = -0.68; 95% confidence level), but are weaker than the correlations produced using the winter sea ice maximum. Hence, it appears that at a regional scale the winter maximum in sea ice shows the strongest relationship to MSA in Weddell region ice cores.

3.4 Interpretation of post-1973 MSA-sea ice relationships in the Weddell Sea region

[17] Over the time period covered by satellite sea ice measurements the Weddell region MSA records consistently show a negative correlation with winter sea ice in the Weddell Sea, and positive correlations with winter sea ice in the more distal Amundsen-Bellingshausen Seas. The main source region for MSA in the Weddell Sea region ice cores is unlikely to be the Amundsen-

Bellingshausen Seas as the Antarctic Peninsula acts as a barrier to westerly near-surface atmospheric transport [*Orr et al.*, 2004; *Parish*, 1983]. Backwards trajectory analysis confirms that most of the weather systems affecting the Weddell-region ice core sites have travelled from the Southern Atlantic Ocean across the Weddell Sea [*Noone et al.*, 1999; *Reijmer et al.*, 1999; *Reijmer and van den Broeke*, 2000; *Russell et al.*, 2004]. An exception to this is the Dolleman Island site where airmasses from the Amundsen-Bellingshausen Seas also contribute to snowfall [*Russell et al.*, 2004]. However, MSA experiences a rapid decrease in concentration during atmospheric transport [*Minikin et al.*, 1998] and the very high concentrations of MSA in the Dolleman Island core suggest that MSA is primarily sourced from the adjacent Weddell Sea [*Pasteur et al.*, 1995]. It is likely instead that the positive correlations observed between the Weddell region MSA records and sea ice in the Amundsen-Bellingshausen Seas are an artefact of the strong inverse relationship between sea ice conditions on the eastern and western sides of the Antarctic Peninsula [*Lefebvre and Goosse*, in press; *Yuan and Martinson*, 2001]. Indeed, the NASA sea ice datasets show that negative correlations at greater than 95% confidence exist between winter sea ice conditions in the Weddell Sea and the Amundsen-Bellingshausen Seas.

[18] Thus it appears that in recent decades the amount of MSA deposited at our ice core sites has been reduced during years when winter sea ice has been more extensive in the Weddell Sea. This negative correlation is opposite to the relationship expected if MSA is to be used as a proxy for winter sea ice [*Curran et al.*, 2003]. This could potentially be due to the extensive summer sea ice regime of the Weddell Sea, and the influence that this has on the area available for MSA production and the transport distance to the coast. In the Law Dome region these additional effects on the MSA-sea ice relationship are small as sea ice experiences a near complete retreat to the coast each year. However, their influence can still be seen when the Law Dome MSA record is compared with the NASA sea ice dataset for the western Pacific sector (90ºE – 160ºE). The correlation with SIE_{max} in this sector produces a positive correlation with an r-value of 0.45. When the MSA record is

compared with SIE_{decay} (i.e. the influence of reduced MSA production area due to summer sea ice is accounted for) the positive correlation between ice core MSA and sea ice is increased to 0.60. The negative influence of summer sea ice on the MSA record, both through decreasing the size of the production area and through increasing MSA loss by increasing the transport distance, is also evident in the strong negative correlation between Law Dome MSA and SIE_{min} in the western Pacific sector (r = -0.65).

[19] In the Weddell Sea region we observe a significant negative correlation between ice core MSA and sea ice decay. However, this relationship is not as strong as the negative correlations produced using the winter sea ice maximum. This reduced significance could be viewed as a slight shift towards the expected positive MSA-sea ice relationship (i.e. more Law Dome-like) when the influence of MSA production area is taken into account. However, it is clear that variations in the area available for MSA production are not the dominant environmental signal being recorded by the Weddell-region ice core records. Likewise, the lack of a significant correlation with the summer sea ice minimum indicates that MSA loss during transport over the summer ice pack does not strongly influence the interannual variability of MSA in our ice core records. The similarity of the correlation results produced using measures of both sea ice extent and ice covered area also suggests that variations in MSA production from within the ice pack are unlikely to be a critical factor controlling the MSA signal in ice cores from this region.

[20] Thus, an issue remains that during the satellite era the most significant and regionally consistent correlations found between our ice core MSA records and sea ice in the Weddell Sea are the negative correlations with the winter maximum in sea ice. There is no direct relationship to explain why MSA is reduced at our ice core sites following winters of more extensive sea ice, and it is also clear that this unexpected relationship cannot be explained by the influence of the summer sea ice pack on MSA production area and transport distance. Instead, it may be that the processes

that affect sea ice conditions in the Weddell Sea (such as temperature and wind direction) also influence the delivery of MSA to our ice core sites. This issue is examined further in section 4.3.2.

4. The 20th century

4.1 Correlations with a historical sea ice record

[21] The existence of a historical sea ice record from the northern Weddell Sea allows for a unique opportunity to further test the nature of MSA-sea ice relationships in this region over a much longer time frame than possible using satellite sea ice records. This historical record provides an index of sea ice duration (SID) from the South Orkney Islands [*Murphy et al.*, 1995] (Fig. 1; Fig. 4). The dataset begins in 1903 and is derived from station measurements of the duration of fast-ice at Factory Cove (Signy Island) and Scotia Bay (Laurie Island). SID at the South Orkney Islands is strongly related to the advance and retreat of the Weddell Sea ice pack around the islands each winter. Comparison with satellite sea ice records shows that the South Orkney SID index reflects the larger-scale winter sea ice conditions of the Weddell Sea [*Murphy et al.*, 1995], and thus provides a reliable reconstruction of regional sea ice changes during the pre-satellite era.

[22] Correlations between the ice core MSA records and South Orkney SID were examined using a block bootstrap resampling method (PearsonT software; [*Mudelsee*, 2003]). The bootstrap method involved resampling the bivariate time series to produce simulated time series of the same length, and calculating correlation coefficients for each simulation. By resampling blocks of linearly detrended data persistence over the block length was preserved. Block lengths were selected using the serial correlations of the time series [*Mudelsee*, 2003]. Correlation coefficients are quoted with a 95% confidence interval, calculated from 2000 bootstrap simulations. Correlations are significantly different from zero at the 95% level when the confidence interval does not include zero.

[23] Each of the individual ice core MSA records has a negative correlation with the South Orkney SID record ($r_{\text{Dolleman Is.}}$ = -0.24 [-0.41,-0.05]; $r_{\text{Berkner Is.}}$ = -0.11 [-0.31,0.10]; r_{DML} = -0.23 [-0.40,-0.04]). A Weddell-region stacked MSA record was again constructed to enhance the common regional MSA signal, by averaging the three individual records after they had been normalised over their common 1900-1990 period (Fig. 4a). This stacked MSA record has an improved negative correlation with South Orkney SID (r = -0.34 [-0.50,-0.18]). A moving correlation analysis, using 21-year sliding correlation windows, further shows that the strength of this relationship has not been constant through time (Fig. 4c). Instead, the negative relationship between the Weddell-region stacked MSA record and South Orkney SID was strongest prior to ~1945 and after ~1975.

4.2 Spectral analysis

[24] Visual examination of the 20th century SID and MSA records suggests that there may be some quasi-periodic variability within these records (Fig. 4; [*Murphy et al.*, 1995]). To further examine the variability of MSA and sea ice in the Weddell Sea region, we first carried out spectral analysis on the full 20th century MSA and SID records using the Lomb–Scargle fourier transform combined with the Welch-overlapped-segment-averaging procedure ([*Schulz and Stattegger*, 1997]; results verified using multitaper spectral estimation [*Percival and Walden*, 1993]). An AR(1) red-noise model was used to test spectral significance (REDFIT software; [*Schulz and Mudelsee*, 2002]). The South Orkney SID record shows spectral peaks exceeding the upper 90% chi-squared red noise level at periodicities of approximately 20 years and 7 years (Fig. 5a). The Weddell-region stacked MSA record also shows evidence for spectral power at ~20 year and ~7 year periods, however these peaks fall below 90% significance when the spectra are calculated over the whole 20th century period. The stacked MSA record does display a significant spectral peak at an ~4 year period. The South Orkney SID record also shows some evidence for spectral power at an ~4 year period, but below the 90% threshold level.

[25] Wavelet power spectra [*Torrence and Compo*, 1998] were also used to examine the time evolution of spectral variance in the Weddell Sea region MSA and sea ice records (Fig. 5b,c). The MSA and SID records show clear similarities in their spectral evolution. In particular, both records show similar time periods where variance at ~4 year, ~7 year and ~20 year periods was significant. There are also clear changes in the amount of variance in each of these bands though the 20th century, which would account for their sometimes low significance when spectral analysis was applied over the full 20th century records (Fig. 5a). In order to better evaluate the MSA-sea ice relationships at these shared periodicities, Gaussian filters were applied to each of the Weddell Sea region MSA and sea ice datasets (Analyseries software; [*Paillard et al.*, 1996]; results verified with the Ferraz-Mello filter algorithm using TIMEFRQ software [*Schulz et al.*, 1999]). The frequency range for filtering was targeted to isolate variability in the ~4 year, ~7 year, and ~20 year bands identified from the spectral analysis results (Fig. 5).

[26] Filtering around the ~4 year period (3.8 – 5.3 year range) shows that there are similarities between the variability at this period in the stacked MSA record and South Orkney SID (Fig. 6a). In particular both filtered records show that variability at a period of ~4 years was strongest between ~1945 – 1970. Variability at this time scale is particularly strong at the Dolleman Island site, accounting for 26% of the total variance in this record, and the power of this periodicity appears to decrease with increasing distance from the coast (Table 3). It should also be noted that whilst the Weddell-region stacked MSA record shows similarities with SID variability at this time scale, the ~4-year filters of the individual MSA records show little correspondence between each other, in terms of both phasing and amplitude changes.

[27] In contrast, variance in each of the Weddell-region MSA records at a period of ~7 years (5.9 – 8.3 year range; Fig. 6b) shows a clear correspondence with changes in SID. Generally it is seen that the amplitude of variance in this frequency band was low between ~1925 – 1965, followed by a

period of high amplitude variance between ~1965 – 1990 (i.e. the satellite era). In this frequency band each of the MSA records has a negative correlation with SID, in agreement with our earlier correlation results. Variance on this time scale is strongest at the Berkner Island site (23% variance), which also has the strongest individual correlation with SID in this frequency band (Table 3).

[28] At periods of ~20 years (16.7 – 33.3 year range; Fig. 6c) the Weddell-region stacked MSA record again retains a negative correlation with SID. This negative correspondence is also observed in the Dolleman Island and DML records, however the Berkner Island record shows no clear correspondence with SID at this time scale. It also appears that the amount of variance in this frequency band is higher in the ice core MSA records than in the South Orkney SID record (Table 3).

4.3 Processes influencing Weddell Sea region MSA and sea ice

4.3.1 Variance at a period of ~4 years

[29] Variance with a period of ~4 years is a common feature of recent Antarctic climate records. Sometimes referred to as the quasi-quadrennial cycle [*Venegas and Drinkwater*, 2001], it is a noted feature of the Antarctic Dipole [*Fundel et al.*, 2006; *Venegas et al.*, 2001; *Yuan and Martinson*, 2001] and the Antarctic Circumpolar Wave [*White and Peterson*, 1996], and may be the result of ENSO teleconnections in the Amundsen Sea region of Antarctica [*Yuan*, 2004]. In the Weddell Sea the quasi-quadrennial cycle is evident as a circulation of sea ice anomalies around the Weddell Gyre [*Venegas and Drinkwater*, 2001]. Whilst all of the Weddell-region MSA records display significant variance at periods of ~4 years, their filtered records differ considerably from each other at this timescale. The local nature of the quasi-quadrennial sea ice anomaly as it propagates around the Weddell Gyre would be expected to result in different representations of this signal at different sites around the basin. Furthermore, the localised impact of the quasi-quadrennial cycle would also

account for the decreasing contribution that variance at this frequency makes to the individual ice core records as distance from the coast increases (Table 3). The apparent strengthening of the Weddell Sea quasi-quadrennial cycle between ~1945 – 1970 (Fig. 6a) may also have contributed to the reduced correlation between the South Orkney SID and stacked MSA records during this interval (Fig. 4c).

4.3.2 Variance at a period of ~7 years

[30] The ~7 year cycle has been noted previously in the later decades of South Orkney SID record [*Murphy et al.*, 1995]. It has also been identified in spectral analysis of reanalysis sea level pressure data throughout the Southern Ocean [*Fischer et al.*, 2004]. Variability at a period of ~7 years is also a feature of the multivariate chemical record of the Siple Dome ice core, which is sensitive to changes in the strength of the low pressure feature over the Amundsen Sea [*Kreutz et al.*, 2000]. The filtering results for this frequency band clearly show that changes in SID and MSA in the Weddell region are linked in both phase (negative) and amplitude (Fig. 6b). It is also clear that variance at a period of ~7 years has not been significant in the Weddell Sea region for the whole of the 20th century (Fig. 5). Instead, variability at this time scale appears to have only dominated Weddell Sea climate between ~1965 – 1990 (Fig. 6b), and thus forms the basis of the negative MSA-winter sea ice relationship identified during the satellite era.

[31] The strong variability in the ~7 year cycle during the NCEP/NCAR reanalysis period [*Kalnay et al.*, 1996; *Marshall and Harangozo*, 2000] allows for the possibility to examine the source of this signal using composite climate anomaly maps. Based on the peaks and troughs in the ~7-year filter of the MSA and SID records composite climate anomaly maps from three years of high sea ice/low MSA conditions were compared to three years of low sea ice/high MSA conditions (Fig. 7). During high sea ice/low MSA years the mean sea level pressure (MSLP) maps show a strengthened Amundsen Sea low pressure anomaly, and a blocking ridge of anomalously high

pressure extending along the Antarctic Peninsula and across the Drake Passage. During low sea ice/high MSA years anomalously high pressure surrounds most of the Antarctic continent, including an anomalous increase in pressure over the Weddell Sea/southern Atlantic Ocean.

[32] The associated meridional wind and surface air temperature anomalies (Fig. 7) provide clues as to why MSA and winter sea ice in the Weddell region have a negative correlation in the ~7 year spectral band. During high sea ice/low MSA years anomalous cooling of the Weddell Sea appears to result from strengthened southerly (offshore) wind flow from the Antarctic continent across the central Weddell Sea towards the South Orkney Islands. This scenario would be expected to increase sea ice extent due to cooler temperatures and enhanced northward wind drift, and is consistent with a recent analysis of the atmospheric conditions associated with increased sea ice extent in the Weddell Sea region [*Lefebvre and Goosse*, in press]. At the same time anomalously strong offshore winds would reduce MSA transport to the ice core sites. Conversely, during low sea ice/high MSA years the composite maps show anomalous wind fields driven by the high pressure anomaly in the South Atlantic Ocean that direct warm air in a northerly (onshore) direction across the western Weddell Sea. This situation would be expected to thermodynamically and dynamically reduce sea ice extent, while also enhancing MSA transport from the Weddell Sea towards the ice core sites. It appears that the mountainous barrier of the Antarctic Peninsula [*Parish*, 1983] acts to focus these meridional wind anomalies across the Ronne/Filchner Ice Shelf and Berkner Island, which may explain why variance at an ~7 year periodicity is strongest in the Berkner Island MSA record.

[33] The climate anomaly maps also show strong anomalies in the Amundsen Sea region, consistent with the presence of ~7 year periodicities in the Siple Dome ice core [*Kreutz et al.*, 2000]. It is also interesting to note that our wavelet spectra and filtering results suggest that variance at this period was weak between ~1925 – 1965 as this corresponds to a period when

interannual variability of the El Nino-Southern Oscillation (ENSO) was also weak [*Torrence and Webster*, 1999].

4.3.3 Variance at a period of ~20 years

[34] A similar analysis of the source of the negative MSA-sea ice relationship at an ~ 20 year period is precluded because this longer period variance is not significant (Fig. 5b and 5c) during the time when the NCEP/NCAR reanalysis data is reliable for the Southern Ocean [*Kalnay et al.*, 1996; *Marshall and Harangozo*, 2000]. Variance with a period of ~20 years is difficult to detect in instrumental records from Antarctica due to its long period with respect to the length of climate records. However, proxy records from Antarctica and beyond do commonly show variance at ~20 year periodicities. Sea salt records from the Siple Dome and Law Dome ice cores contain significant variance at periods near 20 years, and have both been interpreted as proxies for atmospheric transport changes, associated with MSLP variations that may be part of the Southern Annual Mode [*Goodwin et al.*, 2004; *Kreutz et al.*, 2000]. In these studies it was also noted that ~20 year periodicities are found in the spectra of southern hemisphere tree-ring records sensitive to mid-latitude temperatures and MSLP, suggesting that this variability may be related to a hemispheric-scale climatic process. Whilst the climate anomaly maps shown for the ~7 year periodicity may not be directly comparable to the processes associated with the ~20 year periodicity, the negative relationship that persists between the Weddell-region MSA and sea ice records at these long time scales suggests that wind direction and air temperature anomalies are likely to have continued to synergistically increase (decrease) sea ice while also decreasing (increasing) the transport of MSA to the ice core sites around the Weddell Sea.

5. Implications for MSA reconstructions of sea ice

[35] Our comparison of ice core MSA records with satellite sea ice indices since 1973 indicates that the MSA signal retained in near-coastal ice cores around the Weddell Sea shows the strongest

and most regionally consistent correlations with the winter sea ice maximum in the Weddell Sea sector. These correlations show that years of increased sea ice cover are associated with reduced MSA in Weddell Sea region ice core records. This is opposite to the relationship expected if MSA is to be used as a sea ice proxy [*Curran et al.*, 2003], and this difference can not be accounted for by the effect of the summer sea ice pack in the Weddell Sea on MSA production area and transport distance.

[36] Our comparison with a longer historical record of sea ice from the South Orkney Islands confirms the negative relationship that exists with MSA in this region, and identifies characteristic variability at ~4 year, ~7 year, and ~20 year periods in the MSA and sea ice records of this region. Whilst variability at a period of ~4 years is common to all of the MSA records, its expression is quite varied between the individual ice core records suggesting that it may be associated with quasi-quadrennial cycling of local sea ice anomalies around the Weddell Gyre. Variance at the longer ~7 year and ~20 year periods is more consistent between the individual sites, and shows negative correlations with winter sea ice duration at the South Orkney Islands. Reanalysis climate anomaly maps suggest that the negative correlation between sea ice and MSA at the ~7 year period is due to an indirect connection, whereby anomalous cold (warm) air flowing offshore (onshore) across the Weddell Sea acts to increase (decrease) sea ice extent while also decreasing (increasing) the transport of MSA to the ice core sites. A similar examination of the processes associated with variability at an ~20 year period is precluded by the short time span over which the reanalysis data remains reliable for the South Ocean, however the continued negative relationship between MSA and sea ice at this time period suggests that a similar indirect link via wind and air temperature anomalies is likely.

[37] Hence our detailed analysis of ice core MSA records from the Weddell Sea region of Antarctica has shown that in this region ice core MSA records are not a suitable proxy for directly

reconstructing past sea ice conditions. The indirect connection between these records does, however, result in a significant inverse relationship between MSA and sea ice that may have potential for indirectly inferring past sea ice changes in this region. The dominant connection between MSA and onshore/offshore wind strength observed in our Weddell Sea region ice core records appears to also extend further eastward across Dronning Maud Land where a recent study of snow pit and ice core MSA records found that increased MSA concentrations were associated with more efficient atmospheric transport [*Fundel et al.*, 2006]. The pronounced influence that onshore/offshore wind strength appears to have on ice core MSA records in this part of Antarctica is perhaps related to the embayed nature of the Weddell Sea, with the mountainous ridge of the Antarctic Peninsula acting to focus wind anomalies in a north-south direction.

[38] Overall, the potential for ice core MSA records from different sites to reflect sea ice conditions or atmospheric transport strength (or some combination of both) means that great care is needed in assessing their potential to act as proxy records. A multi-proxy approach may help to resolve these issues, with the combined analysis of MSA and other possible chemical indicators of sea ice and atmospheric transport potentially providing a means for assessing the processes dominating observed variability in networks of ice core MSA records from other sites around Antarctica.

Acknowledgments

We thank Mark Curran for making the Law Dome MSA data available for comparison, and for helpful discussions about the interpretation of MSA as a sea ice proxy, and Eugene Murphy for providing the South Orkney SID dataset.

References

Atkinson, A., V. Siegel, P. Evgeny, and P. Rothery (2004), Long-term decline in krill stock and increase in salps within the Southern Ocean, *Nature*, *432*, 100-103.

Cavalieri, D.J., P. Gloersen, C.L. Parkinson, J.C. Comiso, and H.J. Zwally (1997), Observed hemispheric asymmetry in global sea ice changes, *Science*, *278*, 1104-1106.

Comiso, J.C. (1999), *Bootstrap sea ice concentrations for NIMBUS-7 SMMR and DMSP SSM/I, November 1978 - December 2003*, Digital media, updated 2003, available at http://nsidc.org/data/nsidc-0079.html. National Snow and Ice Data Centre, Boulder, CO, USA.

Connolley, W.M. (2005), Sea ice concentrations in the Weddell Sea: A comparison of SSM/I, ULS, and GCM data, *Geophys. Res. Lett.*, *32*, L07501, doi:10.1029/2004GL021898.

Cook, A.J., A.J. Fox, D.G. Vaughan, and J.G. Ferrigno (2005), Retreating glacier fronts on the Antarctic Peninsula over the past half-century, *Science*, *308*, 541-544.

Curran, M.A.J., and G.B. Jones (2000), Dimethyl sulfide in the Southern Ocean: Seasonality and flux, *J. Geophys. Res.*, *105* (D16), 20451-20459.

Curran, M.A.J., A.S. Palmer, T.D. van Ommen, V.I. Morgan, K.L. Phillips, A.J. McMorrow, and P.A. Mayewski (2002), Post-depositional movement of methanesulphonic acid at Law Dome, Antarctica, and the influence of accumulation rate, *Annals of Glaciology*, *35*, 333-339.

Curran, M.A.J., T.D. van Ommen, V.I. Morgan, K.L. Phillips, and A.S. Palmer (2003), Ice core evidence for Antarctic sea ice decline since the 1950s, *Science*, *302*, 1203-1206.

de la Mare, W.K. (1997), Abrupt mid-twentieth-century decline in Antarctic sea-ice extent from whaling records, *Nature*, *389*, 57-60.

Fischer, H., F. Traufetter, R. Oerter, R. Weller, and H. Miller (2004), Prevalence of the Antarctic Circumpolar Wave over the last two millenia recorded in Dronning Maud Land ice, *Geophys. Res. Lett.*, *31*, L08202, doi:10.1029/2003GL019186.

Fundel, F., H. Fischer, R. Weller, F. Traufetter, H. Oerter, and H. Miller (2006), Influence of large-scale teleconnection patters on methane sulfonate ice core records in Dronning Maud Land, *J. Geophys. Res.*, *111*, D04103.

Goodwin, I.D., T.D. van Ommen, M.A.J. Curran, and P.A. Mayewski (2004), Mid latitude winter climate variability in the South Indian and southwest Pacific regions since 1300 AD, *Climate Dynamics*, *22*, 783-794.

Hofstede, C.E., R.S.W. van de Wal, K.A. Kaspers, M.R. van den Broeke, L. Karlof, J.-G. Winther, E. Isaksson, G. Lappegard, R. Mulvaney, H. Oerter, and F. Wilhelms (2004), Firn accumulation records for the past 1000 years on the basis of dielectric profiling of six cores from Dronning Maud Land, Antarctica, *Journal of Glaciology*, *50* (169), 279 - 291.

Jacka, T.H. (1990), Antarctic and Southern Ocean sea-ice and climate trends, *Annals of Glaciology*, *14*, 127-130. Data available at http://www.antcrc.utas.edu.au/~jacka/seaice.html.

Kalnay, E., M. Kanamitsu, R. Kistler, W. Collins, D. Deaven, L. Gandin, M. Iredell, S. Saha, J. Woollen, Y. Zhu, M. Chelliah, W. Ebisuzaki, W. Higgins, J. Janowiak, K.C. Mo, C. Ropelewski, J. Wang, A. Leetmaa, R. Reynolds, R. Jenne, and D. Joseph (1996), The NCEP/NCAR Reanalysis 40-year project, *Bulletin of the American Meterological Society*, *77* (3), 437-471.

Kawaguchi, S., N. Kasamatsu, S. Watanabe, T. Odate, M. Fukuchi, and S. Nicol (2005), sea ice changes inferred from methanesulphonic acid (MSA) variation in East Antarctic ice cores: are krill responsible?, *Antarctic Science*, *17* (2), 211-212, doi: 10.1017/S0954102005002610.

Kreutz, K.J., P.A. Mayewski, I.I. Pittalwala, L.D. Meeker, M.S. Twickler, and S.I. Whitlow (2000), Sea level pressure variability in the Amundsen Sea region inferred from a West Antarctic glaciochemical record, *J. Geophys. Res.*, *105* (D3), 4047-4059.

Lefebvre, W., and H. Goosse (in press), An analysis of the atmospheric processes driving the large-scale winter sea-ice variability in the Southern Ocean, *J. Geophys. Res.*

Marshall, G.J., and S.A. Harangozo (2000), An appraisal of NCEP/NCAR reanalysis MSLP data viability for climate studies in the South Pacific, *Geophys. Res. Lett.*, *27*, 3057 - 3060.

Minikin, A., M. Legrand, J. Hall, D. Wagenbach, C. Kleefeld, E. Wolff, E.C. Pasteur, and F. Ducroz (1998), Sulfur-containing species (sulphate and methansulphonate) in coastal Antarctic aerosol and precipitation, *J. Geophys. Res.*, *103* (D9), 10975-10990.

Minikin, A., D. Wagenbach, W. Graf, and J. Kipfstuhl (1994), Spatial and temporal variations of the snow chemistry at the central Filchner-Ronne Ice Shelf, Antarctica., *Annals of Glaciology*, *20*, 283-290.

Mudelsee, M. (2003), Estimating Pearson's correlation coefficient with bootstrap confidence interval from serially dependent time series, *Mathematical Geology*, *35* (6), 651-665.

Mulvaney, R., H. Oerter, D.A. Peel, W. Graf, C. Arrowsmith, E.C. Pasteur, B. Knight, C. Littot, and W.D. Miners (2002), 1000 year ice-core records from Berkner Island, Antarctica, *Annals of Glaciology*, *35*, 45-51.

Mulvaney, R., E.C. Pasteur, D.A. Peel, E.S. Saltzman, and P.-Y. Whung (1992), The ratio of MSA to non-sea-salt sulphate in Antarctic Peninsula ice cores, *Tellus*, *44B*, 295-303.

Mulvaney, R., and D.A. Peel (1988), Anions and cations in ice cores from Dolleman Island and the Palmer Land plateau, Antarctic Peninsula, *Annals of Glaciology*, *10*, 121-125.

Murphy, E.J., A. Clarke, C. Symon, and J. Priddle (1995), Temporal variation in Antarctic sea-ice: analysis of a long term fast-ice record from the South Orkney Islands, *Deep-Sea Res. I*, *42* (7), 1045-1062.

Noone, D., J. Turner, and R. Mulvaney (1999), Atmospheric signals and characteristics of accumulation in Dronning Maud Land, Antarctica, *J. Geophys. Res.*, *104* (D16), 19191-19211.

Orr, A., D. Cresswell, G.J. Marshall, J.C.R. Hunt, J. Sommeria, C.G. Wang, and M. Light (2004), A 'low-level' explanation for the recent large warming trend over the western Antarctic Peninsula involving blocked winds and changes in zonal circulation, *Geophys. Res. Lett.*, *30*, L06204, doi: 10.1029/2003GL019160.

Paillard, D., L. Labeyrie, and P. Yiou (1996), Macintosh program performs time-series analysis, *EOS transactions, AGU*, *77* (39), 379.

Parish, T.R. (1983), The influence of the Antarctic Peninsula on the wind field over the western Weddell Sea, *J. Geophys. Res.*, *88* (C4), 2684-2692.

Parkinson, C.L. (2004), Southern ocean sea ice and its wider linkages: insights revealed from models and observations, *Antarctic Science*, *16* (4), 387-400, doi: 10.1017/S0954102004002214.

Pasteur, E.C., and R. Mulvaney (2000), Migration of methane sulphonate in Antarctic firn and ice, *J. Geophys. Res.*, *105* (D9), 11525-11534.

Pasteur, E.C., R. Mulvaney, D.A. Peel, E.S. Saltzman, and P.-Y. Whung (1995), A 340 year record of biogenic sulphur from the Weddell Sea area, Antarctica, *Annals of Glaciology*, *21*, 169-174.

Percival, D.B., and A.T. Walden (1993), *Spectral analysis for physical applications: Multitaper and conventional univariate techniques*, 583 pp., Cambridge University Press, New York.

Ravishankara, R.A., Y. Rudich, R. Talukdar, and S.B. Barone (1997), Oxidation of atmospheric reduced sulphur compounds: perspective from laboratory studies, *Philisophical Transactions of the Royal Society of London Series B*, *352*, 171-182.

Rayner, N.A., D.E. Parker, E.B. Horton, C.K. Folland, L.V. Alexander, D.P. Rowell, E.C. Kent, and A. Kaplan (2003), Global analysis fo sea surface temperature, sea ice, and night marine air temperature since the late nineteenth century, *J. Geophys. Res.*, *108* (D14), 4407, doi: 10.1029/2002JD002670.

Reijmer, C.H., W. Greuell, and J. Oerlemans (1999), The annual cycle of meteorolgical variables and the surface energy balance on Berkner Island, Antarctica, *Annals of Glaciology*, *29*, 49-54.

Reijmer, C.H., and M.R. van den Broeke (2000), Moisture sources of precipitation in Western Dronning Maud Land, Antarctica, *Antarctic Science*, *13* (2), 210-220.

Russell, A., G.R. McGregor, and G.J. Marshall (2004), An examination of the precipitation delivery mechanisms for Dolleman Island, eastern Antarctic Peninsula, *Tellus*, *56A*, 501-513.

Saigne, C., and M. Legrand (1987), Measurements of methanesulphonic acid in Antarctic ice, *Nature*, *330*, 240-242.

Schulz, M., W.H. Berger, M. Sarnthein, and P.M. Grootes (1999), Amplitude variations of 1470-year climate oscillations during the last 100,000 years linked to fluctuations of continental ice mass, *Geophys. Res. Lett.*, *26* (22), 3385-3388.

Schulz, M., and M. Mudelsee (2002), REDFIT: estimating red-noise spectra directly from unevenly spaced paleoclimatic time series, *Computers and Geosciences*, *28*, 421-426.

Schulz, M., and K. Stattegger (1997), SPECTRUM: Spectral analysis of unevenly spaced paleoclimatic time series, *Computers and Geosciences*, *23* (9), 929-945.

Sun, J., J. Ren, and D. Qin (2002), 60 years record of biogenic sulfur from Lambert Glacier basin firn core, East Antarctica, *Annals of Glaciology*, *35*, 362-367.

Torrence, C., and G.P. Compo (1998), A practical guide to wavelet analysis, *Bulletin of the American Meterological Society*, *79*, 61-78.

Torrence, C., and P.J. Webster (1999), Interdecadal changes in the ENSO-monsoon system, *J. Clim.*, *12*, 2679-2690.

Vaughan, D.G., G.J. Marshall, W.M. Connolley, C. Parkinson, R. Mulvaney, G. Hodgson, J.C. King, C.J. Pudsey, and J. Turner (2003), Recent rapid regional climate warming on the Antarctic Peninsula, *Climatic Change*, *60*, 243-274.

Venegas, S.A., and M.R. Drinkwater (2001), Sea ice, atmosphere and upper ocean variability in the Weddell Sea, Antarctica, *J. Geophys. Res.*, *106* (C8), 16747-16765.

Venegas, S.A., M.R. Drinkwater, and G. Shaffer (2001), Coupled oscillations in Antarctic sea ice and atmosphere in the South Pacific sector, *Geophys. Res. Lett.*, *28* (17), 3301-3304.

von Storch, H., and F.W. Zwiers (1999), *Statistical analysis in climate research*, 484 pp., Cambridge University Press, Cambridge, UK.

Welch, K.A., P.A. Mayewski, and S.I. Whitlow (1993), Methanesulphonic acid in coastal Antarctic snow related to sea-ice extent, *Geophys. Res. Lett.*, *20* (6), 443-446.

White, W.B., and R.G. Peterson (1996), An Antarctic circumpolar wave in surface pressure, wind, temperature and sea-ice extent, *Nature*, *380*, 699-702.

Wolff, E., H. Fischer, F. Fundel, U. Ruth, B. Twarloh, G.C. Littot, R. Mulvaney, R. Rothlisberger, M. de Angelis, C.F. Boutron, M. Hansson, U. Jonsell, M.A. Hutterli, F. Lambert, P. Kaufmann, B. Stauffer, T.F. Stocker, J.P. Steffensen, M. Bigler, M.L. Siggaard-Andersen, R. Udisti, S. Becagli, E. Castellano, M. Severi, D. Wagenbach, C. Barbante, P. Gabrielli, and V. Gaspari (2006), Southern Ocean sea-ice extent, productivity and iron flux over the past eight glacial cycles, *Nature*, *440*, 491-496, doi:10.1038/nature04614.

Wolff, E., A.M. Rankin, and R. Rothlisberger (2003), An ice core indicator of Antarctic sea ice production?, *Geophys. Res. Lett.*, *30* (22), 2158, doi:10.1029/2003GL018454.

Yuan, X. (2004), ENSO-related impacts on Antarctic sea ice: a synthesis of phenomenon and mechanisms, *Antarctic Science*, *16* (4), 415-425.

Yuan, X., and D.G. Martinson (2001), The Antarctic Dipole and its predictability, *Geophys. Res. Lett.*, *28* (18), 3609-3612.

Zwally, H.J., J.C. Comiso, C.L. Parkinson, D.J. Cavalieri, and P. Gloersen (2002), Variability of Antarctic sea ice 1979-1998, *J. Geophys. Res.*, *107* (C5), 3041, doi: 10.1029/2000JC000733.

Figure captions

Figure 1. The Weddell Sea region of Antarctica showing the locations of the ice cores used in this study. Inset shows the typical summer (dark shading) and winter (light shading) sea ice extents around Antarctica, and the location of the Law Dome site (L.D.).

Figure 2. Ice core MSA records from the Weddell Sea region since 1973. (a) Records of ice core MSA are shown for Dolleman Island (dashed curve), Berkner Island (black solid curve), and DML (grey curve). Each record was normalised relative to the mean and standard deviation of MSA from 1973 – 1990 (Table 1), with higher normalised values representing increased MSA concentration. (b) A Weddell-region stacked MSA record was derived from the three individual ice core MSA records. Error bars show the standard error for each annual value of the stacked MSA record.

Figure 3. Correlation of ice core MSA records from the Weddell Sea region with 10º sectors of SIE since 1973. (a) The Weddell-region stacked MSA record shows a broad region of negative correlations with SIE_{max} in the Weddell Sea and a positive correlation with SIE_{max} in the Amundsen/Bellingshausen Seas. Correlations are based on unsmoothed, annual resolution data, and significance estimations (2-tailed t-test) include corrections for serial correlation within the datasets. Values marked with * and ** represent correlations that are significant at 90% and 95% levels, respectively. Red circles show the locations of the three ice cores used to create the stacked MSA record. (b) The three individual MSA records (Dolleman Island = dashed curve; Berkner Island = black solid curve; DML = grey curve) all display similar correlation patterns with SIE_{max}. Correlations of the Weddell-region stacked MSA record with (c) SIE_{min}, and (d) SIE_{decay} are also shown. Correlation and significance details for panels (c) and (d) as in panel (a).

Figure 4. Comparison of ice core MSA records from the Weddell Sea region with sea ice duration at the South Orkney Islands. (a) A stacked Weddell-region MSA record was produced from the average of the three individual ice core records normalised over the common 1900-1990 period. The stacked record is shown with a 3-year smooth, and error bars show the standard error for each yearly value. (b) The South Orkney SID record has been normalised over the 1903-1990 period, and smoothed with a 3-year running mean. Higher normalised values represent (a) higher MSA concentrations and (b) longer winter sea ice duration. Over the 20th century the unsmoothed Weddell-region stacked MSA record has a negative correlation with SID at the South Orkney Islands (r = -0.34 [-0.50,-0.18]; [*Mudelsee*, 2003]). (c) 21-year moving correlation coefficients (black circles) of the South Orkney SID with the Weddell-region stacked MSA record show that this negative relationship was strongest during the first half of the 20th century. Dashed lines show the 95% confidence interval, computed using bootstrap methods (1000 sample Monte Carlo; computed at http://climexp.knmi.nl/).

Figure 5. Spectral analysis of the Weddell Sea region MSA and sea ice records. (a) The Lomb-Scargle spectra are shown for the 20th century records of South Orkney SID (dark grey shading) and the Weddell-region stacked MSA record (black curve). Spectra were calculated using 3 overlapping (50%) segments, linear detrending, and a Welch I data taper. The spectra have been scaled relative to the upper 90% chi-squared AR(1) red-noise bound [*Schulz and Mudelsee*, 2002], such that significant spectral peaks have values greater than 1 (i.e. above the cross-hatched region). This scaling method allows for a clearer comparison of the different spectra and their significant peaks, however it results in the loss of the typical red-noise shape of the spectra where lower frequencies have higher power. Significant peaks occur at 19 and 7-year periods in the South Orkney SID record, and at a 4.4-year period in the Weddell-region stacked MSA record. Wavelet power spectra [*Torrence and Compo*, 1998] show the time evolution of variance for (b) the South Orkney SID record and (c) the Weddell-region stacked MSA record. The contour levels are chosen

so that 75%, 50%, 25%, and 5% of the wavelet power is above each level, respectively (blue to red). Black contour is the 90% confidence level, using a red-noise AR(1) background spectrum. The cross-hatched region is the cone of influence, where zero padding at the ends of the datasets has reduced the variance. There are clear similarities between the wavelet spectra of the SID and stacked MSA records, and each shows times of significant variance at ~4 year, ~7 year and ~20 year periods.

Figure 6. Gaussian filters of variance in the Weddell-region MSA and sea ice records. The South Orkney SID (shaded grey curve) and Weddell-region stacked MSA (black curve) records were filtered to examine the characteristics of their variance at periods of, (a) 3.8 – 5.3 years (frequency, $f = 0.225 \pm 0.035$ years^{-1}), (b) 5.9 – 8.3 years ($f = 0.145 \pm 0.025$ years^{-1}) and, (c) 14.3 – 25 years ($f = 0.055 \pm 0.015$ years^{-1}). Frequency bands for filtering were selected using the spectral analysis results in Fig. 5, and filtering was carried out using Analyseries software [*Paillard et al.*, 1996]. Note that the filtered records of Weddell-region stacked MSA in panels (b) and (c) are shown on an inverted scale due to their strong negative correlation with SID (Table 3).

Figure 7. Climate anomaly maps for extreme years in the ~7 year variability band. Composite anomaly maps of mean sea level pressure (MSLP), 850mb zonal wind, 850mb meridional wind, and surface air temperature (SAT) were constructed for years of high SID / low MSA (left side column; years ending 1974, 1981 and 1988), years of low SID / high MSA (central column; years ending 1971, 1978 and 1985), and for the difference between these extreme years (high SID minus low SID years; right side column). Anomalies represent averages running from July to June, so as to incorporate the austral winter SID anomaly and the following summer MSA anomaly. Climate anomaly maps from the NCEP/NCAR reanalysis data [*Kalnay et al.*, 1996], provided by the NOAA-ESRL Physical Sciences Division from their web site at http://www.cdc.noaa.gov/

Tables

Table 1. Site location and details for the ice cores used in this study.

Core	Collection year	Location	Accumulation rate (m.w.e.)	Surface elevation (m)	Distance from coast (km)	Mean (& s.d.) of MSA, 1973 to 1990 (ppb)
Dolleman Island	1985/86 & 1992/93	70º35'S 060º56'W	0.34	398	20	55.4 (26.4)
Berkner Island (north dome)	1994/95	78º19'S 046º17'W	0.20	718	50	16.6 (9.1)
Dronning Maud Land	1997/98	77º03'S 010º30'W	0.065	2180	460	4.9 (2.9)

Table 2. Correlation coefficients (r) between Weddell Sea ice core MSA records and NASA sea ice data. Correlations are based on unsmoothed, annual resolution data, and significance estimations (2-tailed t-test) include corrections for serial correlation within the datasets. Values marked with *, ** and *** represent correlations that are significant at 90%, 95% and 99% levels, respectively.

	Weddell Sea (060ºW – 020ºE)		Amundsen-Bellingshausen Seas (140ºW – 060ºW)		Circum-Antarctic mean (0º – 360º)	
Core	SIE_{max}	ICA_{max}	SIE_{max}	ICA_{max}	SIE_{max}	ICA_{max}
Dolleman Island	-0.28	-0.28	0.21	0.15	0.19	0.15
Berkner Island	-0.48	-0.48	0.31	0.25	-0.20	-0.31
DML	-0.54*	-0.57**	0.59**	0.66**	-0.64**	-0.36
Weddell stack	-0.76**	-0.78***	0.62*	0.62*	-0.45	-0.40

Table 3. Gaussian filtering results showing the amount of variance explained by each spectral band, and the correlation that each MSA filter has with the corresponding filter of the South Orkney SID record. Due to serial correlation in the filtered record the correlation values should only be used as a guide to the sign and relative strength of the relationship to variance in the South Orkney SID record.

	3.8 – 5.3 year filter ($f = 0.225 \pm 0.035$ y^{-1})		5.9 – 8.3 year filter ($f = 0.145 \pm 0.025$ y^{-1})		14.3 – 25 year filter ($f = 0.055 \pm 0.015$ y^{-1})	
Record	variance	r_{SID}	variance	r_{SID}	variance	r_{SID}
South Orkney SID	15%		16%		9%	
Weddell-region stacked MSA	15%	0.21	20%	-0.69	27%	-0.80
Dolleman Island MSA	26%	0.33	13%	-0.42	21%	-0.85
Berkner Island MSA	15%	-0.05	23%	-0.68	21%	0.09
DML MSA	8%	-0.09	7%	-0.36	31%	-0.62

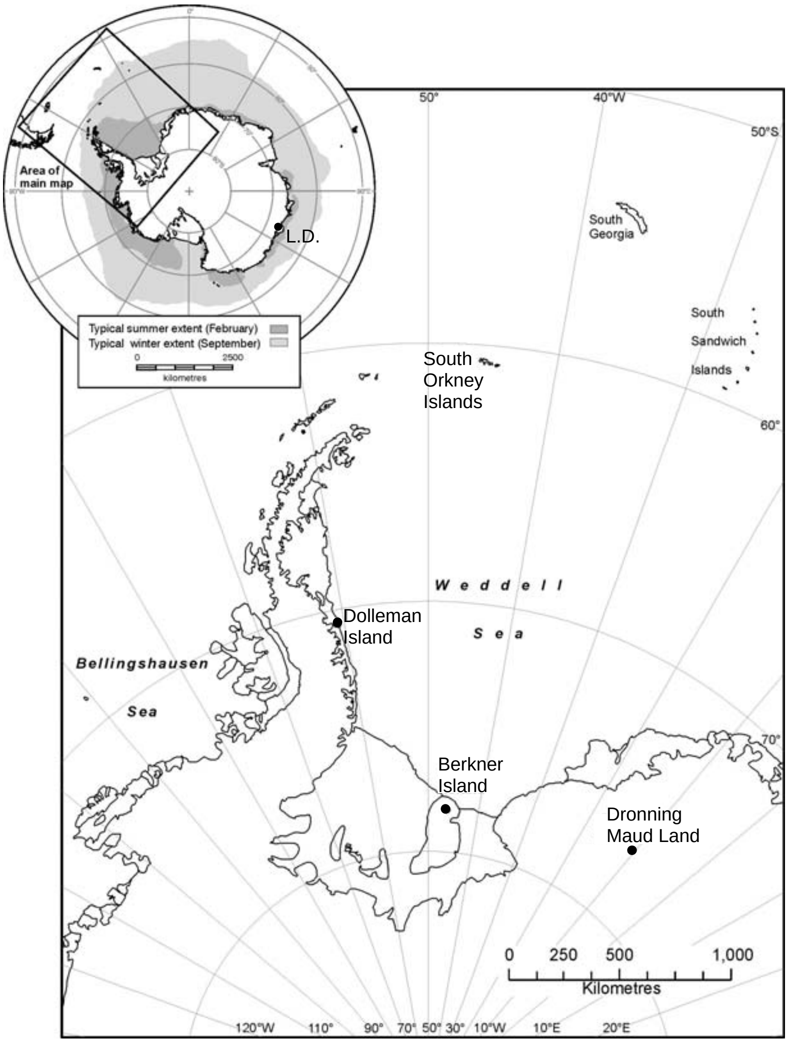

Figure 1. The Weddell Sea region of Antarctica showing the locations of the ice cores used in this study. Inset shows the typical summer (dark shading) and winter (light shading) sea ice extents around Antarctica, and the location of the Law Dome site (L.D.).

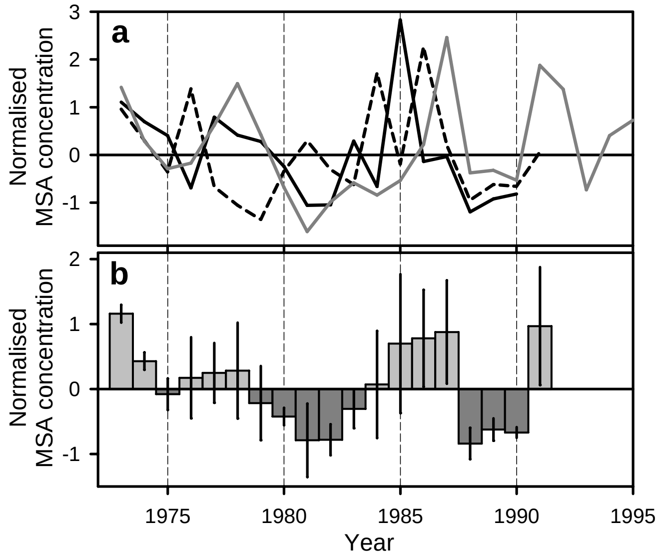

Figure 2. Ice core MSA records from the Weddell Sea region since 1973. (a) Records of ice core MSA are shown for Dolleman Island (dashed curve), Berkner Island (black solid curve), and DML (grey curve). Each record was normalised relative to the mean and standard deviation of MSA from 1973 – 1990 (Table 1), with higher normalised values representing increased MSA concentration. (b) A Weddell-region stacked MSA record was derived from the three individual ice core MSA records. Error bars show the standard error for each annual value of the stacked MSA record.

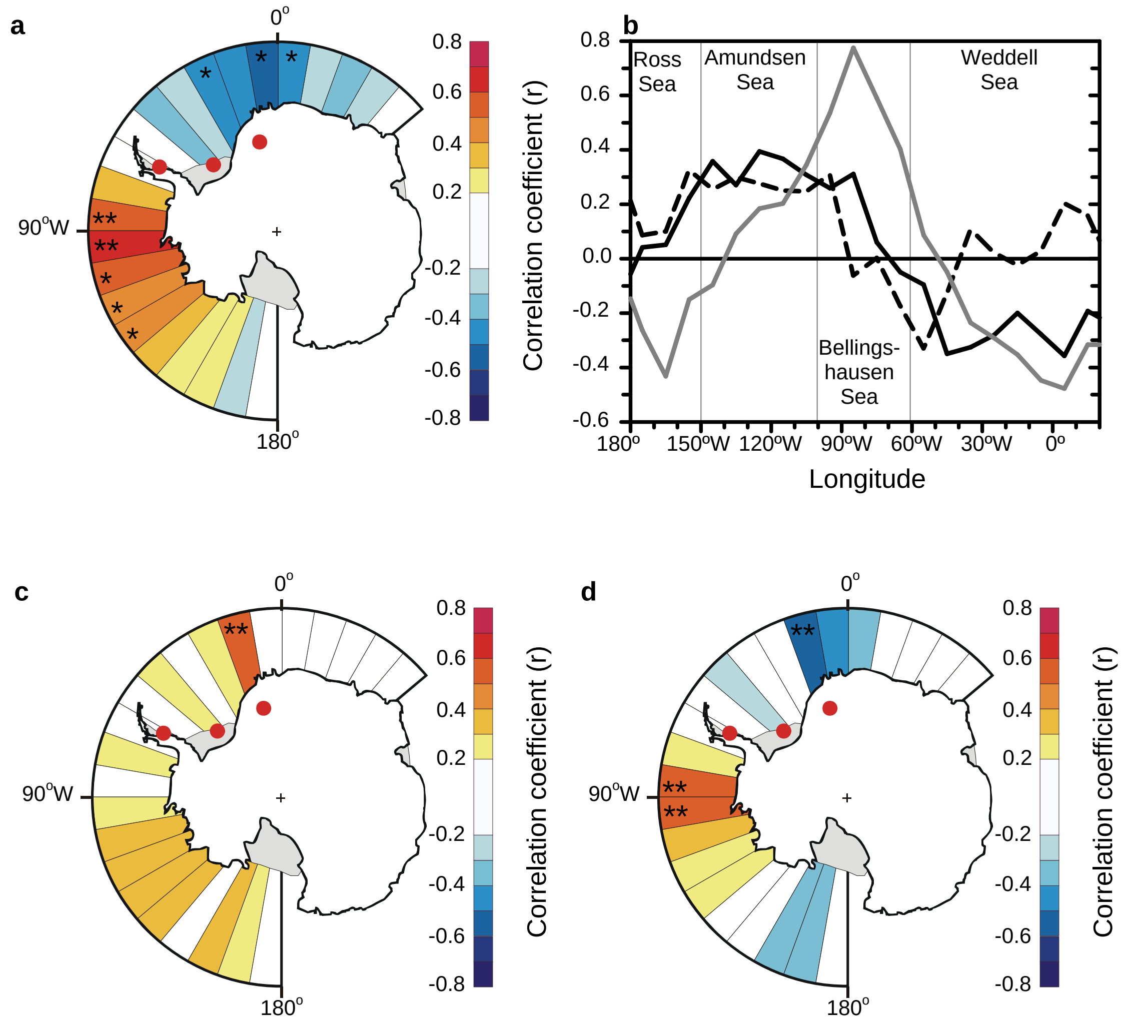

Figure 3. Correlation of ice core MSA records from the Weddell Sea region with 10° sectors of SIE since 1973. (a) The Weddell-region stacked MSA record shows a broad region of negative correlations with SIE_{max} in the Weddell Sea and a positive correlation with SIE_{max} in the Amundsen/Bellingshausen Seas. Correlations are based on unsmoothed, annual resolution data, and significance estimations (2-tailed t-test) include corrections for serial correlation within the datasets. Values marked with * and ** represent correlations that are significant at 90% and 95% levels, respectively. Red circles show the locations of the three ice cores used to create the stacked MSA record. (b) The three individual MSA records (Dolleman Island = dashed curve; Berkner Island = black solid curve; DML = grey curve) all display similar correlation patterns with SIE_{max}. Correlations of the Weddell-region stacked MSA record with (c) SIE_{min}, and (d) SIE_{decay} are also shown. Correlation and significance details for panels (c) and (d) as in panel (a).

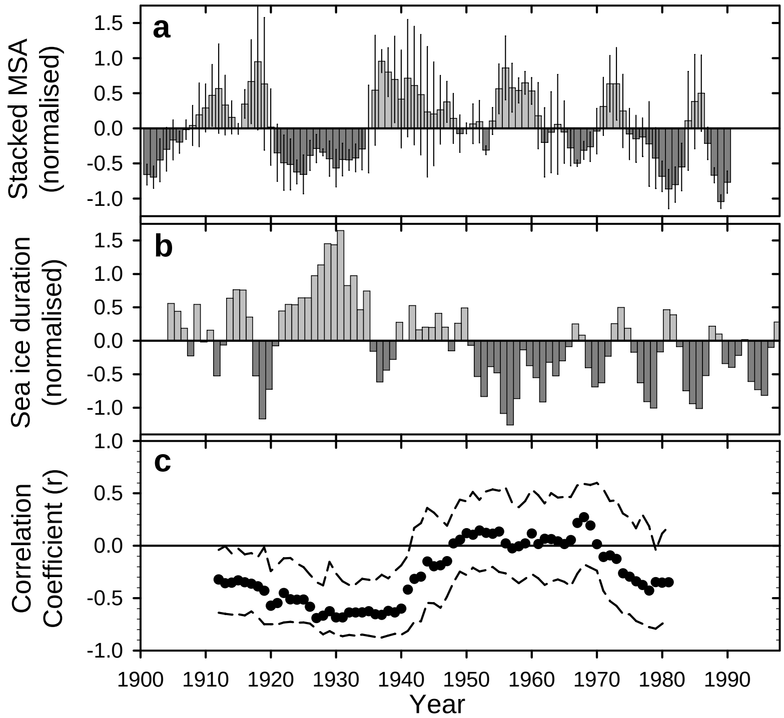

Figure 4. Comparison of ice core MSA records from the Weddell Sea region with sea ice duration at the South Orkney Islands. (a) A stacked Weddell-region MSA record was produced from the average of the three individual ice core records normalised over the common 1900-1990 period. The stacked record is shown with a 3-year smooth, and error bars show the standard error for each yearly value. (b) The South Orkney SID record has been normalised over the 1903-1990 period, and smoothed with a 3-year running mean. Higher normalised values represent (a) higher MSA concentrations and (b) longer winter sea ice duration. Over the 20th century the unsmoothed Weddell-region stacked MSA record has a negative correlation with SID at the South Orkney Islands (r = -0.34 [-0.50,-0.18]; [*Mudelsee*, 2003]). (c) 21-year moving correlation coefficients (black circles) of the South Orkney SID with the Weddell-region stacked MSA record show that this negative relationship was strongest during the first half of the 20th century. Dashed lines show the 95% confidence interval, computed using bootstrap methods (1000 sample Monte Carlo; computed at http://climexp.knmi.nl/).

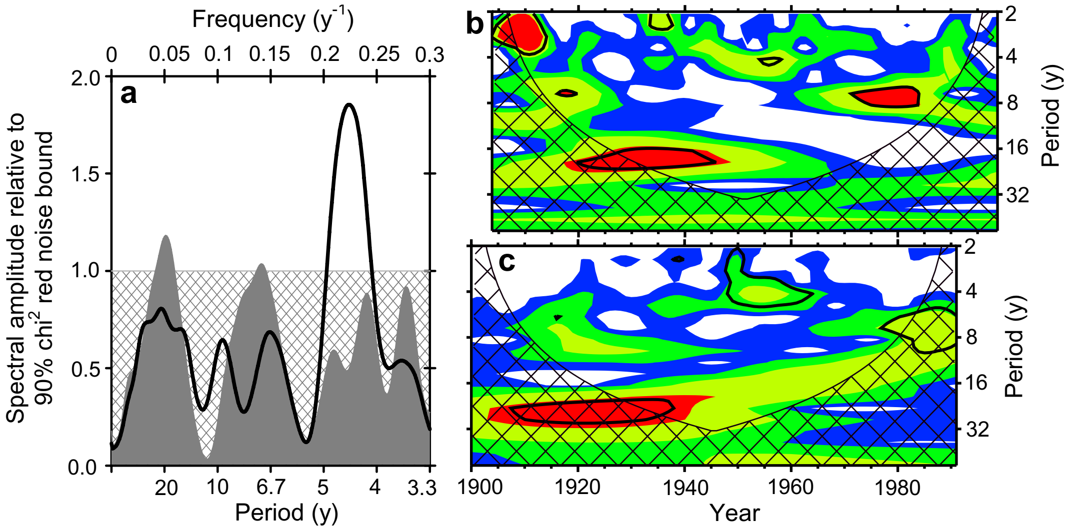

Figure 5. Spectral analysis of the Weddell Sea region MSA and sea ice records. (a) The Lomb-Scargle spectra are shown for the 20th century records of South Orkney SID (dark grey shading) and the Weddell-region stacked MSA record (black curve). Spectra were calculated using 3 overlapping (50%) segments, linear detrending, and a Welch I data taper. The spectra have been scaled relative to the upper 90% chi-squared AR(1) red-noise bound [*Schulz and Mudelsee*, 2002], such that significant spectral peaks have values greater than 1 (i.e. above the cross-hatched region). This scaling method allows for a clearer comparison of the different spectra and their significant peaks, however it results in the loss of the typical red-noise shape of the spectra where lower frequencies have higher power. Significant peaks occur at 19 and 7-year periods in the South Orkney SID record, and at a 4.4-year period in the Weddell-region stacked MSA record. Wavelet power spectra [*Torrence and Compo,* 1998] show the time evolution of variance for (b) the South Orkney SID record and (c) the Weddell-region stacked MSA record. The contour levels are chosen so that 75%, 50%, 25%, and 5% of the wavelet power is above each level, respectively (blue to red). Black contour is the 90% confidence level, using a red-noise AR(1) background spectrum. The cross-hatched region is the cone of influence, where zero padding at the ends of the datasets has reduced the variance. There are clear similarities between the wavelet spectra of the SID and stacked MSA records, and each shows times of significant variance at ~4 year, ~7 year and ~20 year periods.

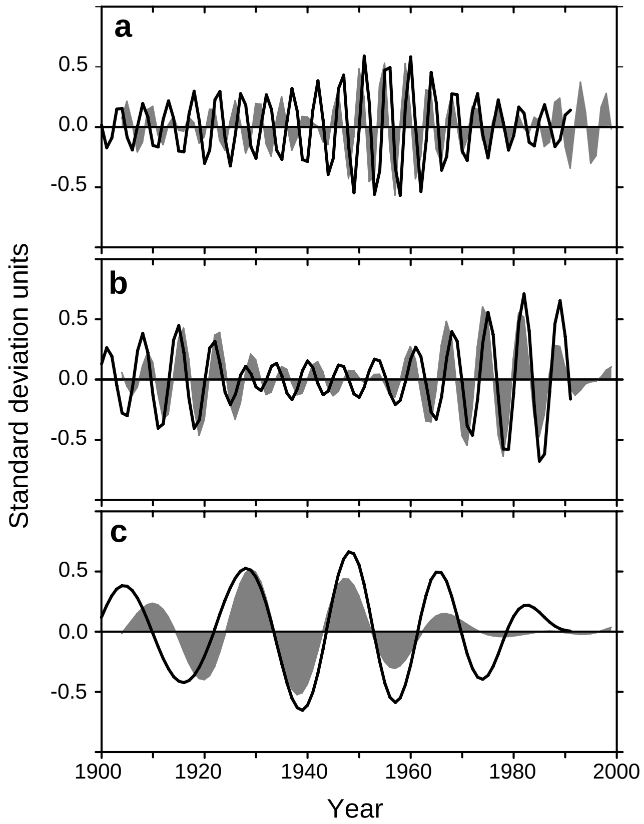

Figure 6. Gaussian filters of variance in the Weddell-region MSA and sea ice records. The South Orkney SID (shaded grey curve) and Weddell-region stacked MSA (black curve) records were filtered to examine the characteristics of their variance at periods of, (a) 3.8 – 5.3 years (frequency, $f = 0.225 \pm 0.035$ years^{-1}), (b) 5.9 – 8.3 years ($f = 0.145 \pm 0.025$ years^{-1}) and, (c) 14.3 – 25 years ($f = 0.055 \pm 0.015$ years^{-1}). Frequency bands for filtering were selected using the spectral analysis results in Fig. 5, and filtering was carried out using Analyseries software [*Paillard et al.*, 1996]. Note that the filtered records of Weddell-region stacked MSA in panels (b) and (c) are shown on an inverted scale due to their strong negative correlation with SID (Table 3).

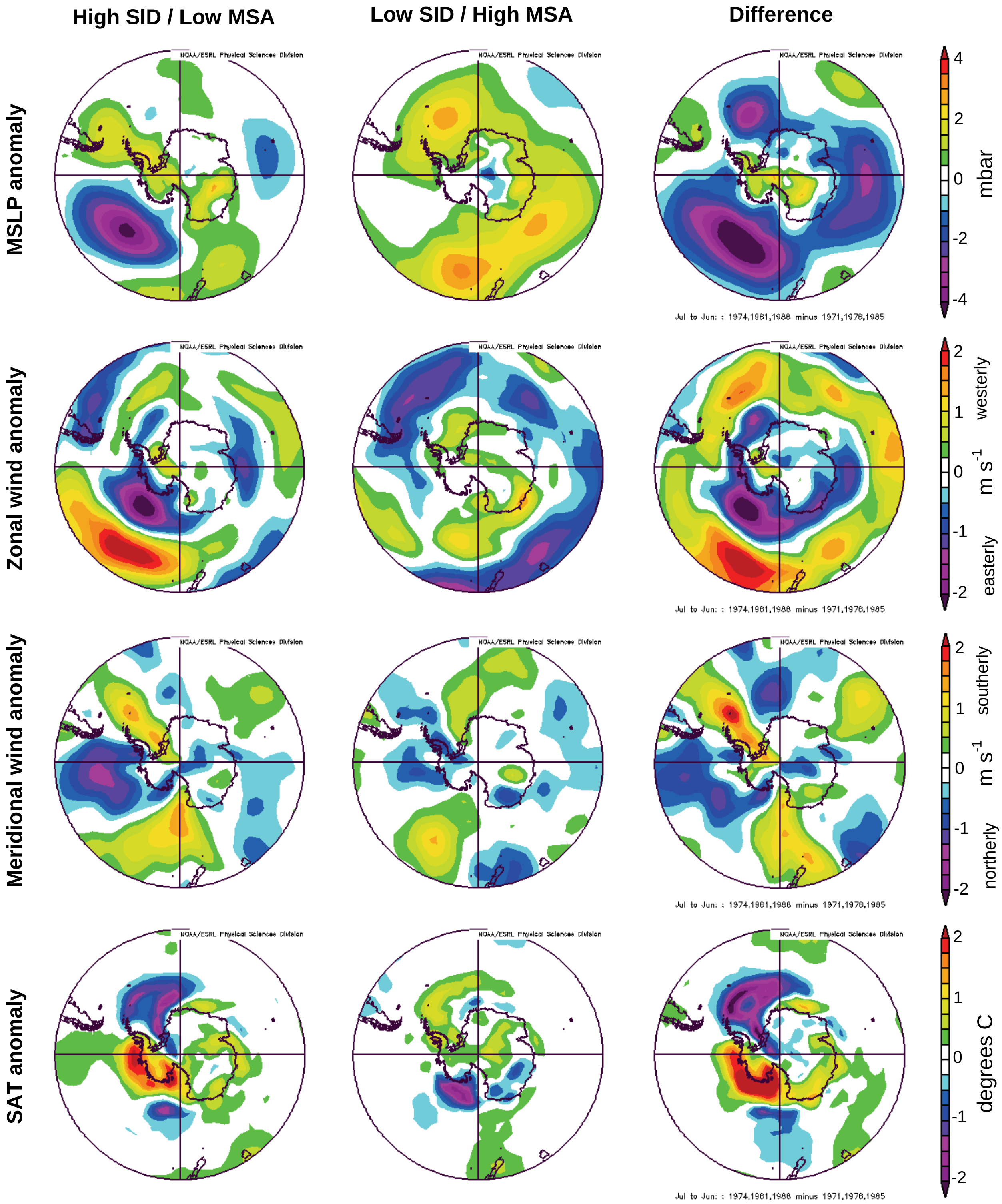

Figure 7. Climate anomaly maps for extreme years in the ~7 year variability band. Composite anomaly maps of mean sea level pressure (MSLP), 850mb zonal wind, 850mb meridional wind, and surface air temperature (SAT) were constructed for years of high SID / low MSA (left side column; years ending 1974, 1981 and 1988), years of low SID / high MSA (central column; years ending

1971, 1978 and 1985), and for the difference between these extreme years (right side column). Anomalies represent averages running from July to June, so as to incorporate the austral winter SID anomaly and the following summer MSA anomaly. Climate anomaly maps from the NCEP/NCAR reanalysis data [*Kalnay et al.*, 1996], provided by the NOAA-ESRL Physical Sciences Division from their web site at http://www.cdc.noaa.gov/